

*Special Issue: Artificial Intelligence*

*Scientific Paper*

Doi: <http://dx.doi.org/10.1590/1809-4430-Eng.Agric.v42nepe20210123/2022>

## COMPUTATIONAL INTELLIGENCE APPLIED IN OPTIMAL DESIGN OF WOODEN PLANE TRUSSES

**André L. Christoforo<sup>1</sup>, Matheus H. M. de Moraes<sup>1\*</sup>, Iuri F. Fraga<sup>1</sup>,  
Wanderlei M. Pereira Junior<sup>2</sup>, Francisco A. R. Lahr<sup>3</sup>**

<sup>1\*</sup>Corresponding author. Federal University of Sao Carlos/ Sao Carlos - SP, Brazil.

E-mail: [matheus.h.h@hotmail.com](mailto:matheus.h.h@hotmail.com) | ORCID ID: <https://orcid.org/0000-0002-7285-1344>

### KEYWORDS

computational intelligence, optimization, timber truss, dicotyledonous.

### ABSTRACT

The use of wood is widespread in rural constructions, and the truss systems stand out among its various applications. This specific system has several typologies and requires a thorough study to determine the most advantageous model for each project. The present study aims to apply the Computational Intelligence concepts to determine the minimum viable cross-section of a Howe truss. For the computational simulation, methods like Finite Elements were used to obtain the loads and the Firefly Algorithm for the optimization process, focusing on minimizing the total weight of the structural part. Studies were conducted varying the spans of the elements and the height to span ratio. The design assumptions for establishing the optimization method's constraints follow the recommendations of the Brazilian standard for wood design, ABNT NBR 7190 (1997). Weights between 95.42 kg and 653.57 kg were obtained, and all optimization processes presented feasible solutions for the design constraints.

### INTRODUCTION

The emergence of novel technologies has facilitated the development of optimized installations increasing the structural performance in a service. These performance requirements are desired in urban as well as rural constructions (Chrisp et al., 2003; Tahsildoost & Zomorodian, 2020).

In rural buildings, wood is an attractive alternative material for improving energy efficiency in construction (Hens et al., 2021). Within such applications, the wooden trusses are some of the most used elements in constructing roofing systems (Krušínský et al., 2017; Z. Li et al., 2019), existing several typologies for this purpose.

The design of roof structures is a complex process with several verifications. Numerous variables in the structural design process has led to the popularization of metaheuristic optimization, a branch of computational mathematics.

Metaheuristic optimization is understood in the context of computational intelligence, a set of numerical tools using algorithms that reproduce the social behavior of animals (Zhang et al., 2013; Darwish, 2018; Salehi & Burgueño, 2018; Nguyen et al., 2020). In the artificial intelligence literature, these algorithms are presented as boosting algorithms due to their ability to interact with the environment and obtain information for decision making in subsequent iterations (Whitley et al., 1994; Ding et al., 2019).

Such methods simulate an animal's social behavior and natural intelligence, for example: (a) Genetic Algorithms (GA); (b) Particle Swarm Optimization (PSO); and (c) Firefly Algorithm (FA), which is the focus of this paper. These algorithms have been employed in various scientific fields, including stock market (Kumar & Mishra, 2017), image processing (Hoang, 2019), inverse problems (Raecker et al., 2019; Pereira Junior et al., 2021), etc.

<sup>1</sup> Federal University of Sao Carlos/ Sao Carlos - SP, Brazil.

<sup>2</sup> Federal University of Catalao/ Catalao - GO, Brazil.

<sup>3</sup> University of São Paulo/ Sao Carlos - SP, Brazil.

Area Editor: Adão Felipe dos Santos

Received in: 7-31-2021

Accepted in: 1-4-2022

Structural optimization has become a viable tool, applied to various structural engineering problems including sizing, such as timber beams (Pech et al., 2019; Mayencourt & Mueller, 2020; Schietzold et al., 2021), wooden frame structures (Mam et al., 2020), and wooden trusses (Villar et al., 2016; Villar-García et al., 2019). These methods can automate the structural sizing process (Assimi et al., 2017; Degertekin et al., 2018; Bianconi et al., 2019), assisting engineers to focus on to the important requirements, such as total cost, durability, and performance.

Several types of trusses can be applied to engineering projects. Therefore, this research aims to use a Computational Intelligence algorithm, FA, for a parametric study of trusses for rural constructions. The optimization problem is based on minimizing the weight of the truss based on the design constraints of the Brazilian standard ABNT NBR 7190 (1997). Despite the references above, most studies related to structural optimization have their applications emphasize concrete and steel. Therefore, this work involves a parametric analysis of trusses, aiming for its application in the design of timber structures, forming a basis for future research.

As stated earlier, the FA algorithm was employed for the same. In literature, FA was used for optimization in several structural systems with different materials, such as steel beam design, steel pressure vessel design, steel helical compression spring design, reinforced concrete beam design, steel cantilever beam design, and steel tower structure design (Gandomi et al., 2011; Talatahari et al., 2014).

Moreover, the FA usage is not restricted to structural engineering problems, but several related engineering areas, such as system identification design problem, location-design problem, groundwater remediation design, construction system reliability analysis, power system design, and antenna design (Ram et al., 2014; Kazemzadeh-Parsi et al., 2015; Y. Li et al., 2016; Sadjadi et al., 2016; Setiadi & Jones, 2016; Upadhyay et al., 2016). This corroborates with the FA application to optimize timber truss, the research aim.

## MATERIAL AND METHODS

For the development of this work, the criteria established by the Brazilian standard for timber structures, ABNT NBR 7190 (1997), were considered for the truss design. This section will present the optimization algorithm and the penalization method. The Objective Function (OF) and the details for the parametric study were calculated. And the Finite Element Method (FEM) was used to determine the loads in each bar of the truss and nodal displacements, the FEM was used.

### Algorithm used to optimize truss bars

For truss optimization, FA was used, as developed by Yang (2008). The FA is a bio-inspired algorithm with population characteristics, i.e., two or more particles pass through the sample space seeking an optimal and viable solution. The biological concept used to develop this algorithm including bioluminescence and the interference of iterations during the crossing of fireflies. Thus, FA is based on the ability of fireflies to emit light and population individuals to perceive this light (Yang, 2008).

Conceiving the initial populations, the firefly (or design variable) starts a random walk process, thus the firefly  $\vec{x}$  “moves” according to an update function of the design variables ( $\vec{\omega}$ ) (Equation 1), where  $\vec{x}$  is the vector of design variables,  $\vec{\omega}$  is the update vector function of the design zvariable  $\vec{x}$ , and  $t$  is the number of iterations.

$$\vec{x}^{t+1} = \vec{x}^t + \vec{\omega}^t \quad (1)$$

Based on this new direction, the possible candidate solutions were evaluated for generating the optimal design point (Wang et al., 2017). Thus, the update function of the movement of the fireflies’ iterations is given by [eq. (2)].

$$\omega^t = \beta(\vec{x}_j^t - \vec{x}_i^t) + \alpha(\vec{\eta} - 0,5 \vec{\epsilon}) \quad (2)$$

From [eq. (2)],  $\beta$  is the attractiveness between the fireflies  $i$  and  $j$ ,  $\vec{x}_i$  is the firefly  $i$ ,  $\vec{x}_j$  is the firefly  $j$ ,  $\vec{\eta}$  is the vector of random numbers between 0 and 1,  $\alpha$  is the randomness factor, and  $\vec{\epsilon}$  is a unit vector.

To ensure the randomness of the process, a randomness factor  $\alpha$  is used. Its behavior is described by following an exponential decay behavior according to the number of iterations  $t$ , following the formulation proposed by [eq. (3)], where  $\theta$  is the decay constant equal to 0.98.

$$\alpha = \alpha_{min} + (\alpha_{max} - \alpha_{min}) \cdot \theta^t \quad (3)$$

As described, the term  $\beta$  describes the attractiveness between the fireflies in the population (Equation 4), where  $\beta_0$  is the attractiveness for a distance  $r = 0$ ,  $r_{ij}$  is the Euclidean distance between fireflies  $i$  and  $j$  (Equation 5), and  $\gamma$  is the light absorption parameter (Equation 6).

$$\beta = \beta_0 e^{-\gamma r_{ij}^2} \cong \beta_0 / (1 + \gamma r_{ij}^2) \quad (4)$$

$$r_{ij} = \|\vec{x}_i - \vec{x}_j\| = \sqrt{\sum_{k=1}^d (\vec{x}_{i,k} - \vec{x}_{j,k})^2} \quad (5)$$

$$\gamma = 1 / (x_{max} - x_{min})^2 \quad (6)$$

From eqs (5) and (6),  $k$  is the  $k$ -th component of the vector of design variables  $\vec{x}$ ,  $d$  is the number of design variables,  $x_{max}$  is the top bound of the design variables and  $x_{min}$  is the bottom bound of the design variables.

The algorithm parameters used in the study are presented in

TABLE 1, based on the sensitivity study developed by Pereira et al. (2020).

TABLE 1. FA input parameters.

Parameter	Meaning	Adopted value
$\beta_0$	Attractiveness among fireflies	0.90
$N_{gen}$	Number of generations	500
$N_{pop}$	Population size	20
$\alpha_{min}$	Minimum randomness factor	0.20
$\alpha_{max}$	Maximum randomness factor	1.00
$R_p$	Penalty factor	$10^5$

Pereira et al. (2020) developed a study applying the FA to optimize a steel truss. Notably, Pereira et al. (2020) study regarded the constraints based on the material mechanics, without considering the standard steel design requirements. Moreover, the study did not focus on the typologies and the parametric study. Therefore, the present research contributes to developing the optimization to understand the Howe typology behavior performing a parametric study for this purpose, applying the Brazilian standard for wood design, using their design and calculation precepts.

### OF and treatment of constraints

The present study aims to minimize the total weight of the structural system considering the constraints of nodal displacements, mechanical resistance of the bars, and geometric criteria generating lateral instability in the structural system. The OF of the problem is expressed by [eq. (7)], where  $A_i$  is the cross-section area of bar  $i$ ,  $\rho_i$  is the density of the material,  $L_{0i}$  is the length of the bar  $i$  of the truss, and  $n$  is the number of truss bars.

$$FO(A_i, \rho_i, L_{0i}) = \sum_{i=1}^n A_i \cdot \rho_i \cdot L_{0i} \quad (7)$$

For the constraint treatment procedure, the external penalty technique was used (Kuri-Morales & Gutiérrez-García, 2002; Yeniay, 2005). The OF was modified to obtain a pseudo-objective function, where  $g_j$  and  $h_k$  represent the inequality and equality constraints, respectively. Equation 8 shows the penalty method adopted, and the penalized OF  $W$  is presented in [eq. (9)].

$$P(\vec{x}) = \sum_{j=1}^m \max[0, g_j(\vec{x})]^2 + \sum_{k=1}^n [h_k(\vec{x})]^2 \quad (8)$$

$$W(A_i, \rho_i, L_{0i}, \vec{x}_i) = FO(A_i, \rho_i, L_{0i}) + R_p P(\vec{x}) \quad (9)$$

From [eq. (8)],  $P(\vec{x})$  is the static outer penalty function,  $j$  and  $k$  are  $j$ -th constraints of inequality and  $k$ -th constraints of equality, respectively,  $m$  and  $n$  are the total number of constraints of inequality and equality, respectively,  $\vec{x}$  is the solution vector (random population),  $g$  and  $h$  are the set of constraints of inequality and equality, respectively, and  $W(\vec{x})$  is the penalized OF.

### Description of truss and design variables

For the optimization process, the present work adopted the flat truss of the Howe typology. The group of trusses was divided into seven spans with the lengths of 6, 9, 12, and 15 meters. Thirty optimization process was performed for each truss to obtain a significant dispersion of the results.

FIGURE 1 displays a generic representation of node distances ( $B = L/6$  and  $H$ ), with the bar design and position variables considered  $\vec{x}_1, \vec{x}_2, \vec{x}_3$ , and  $\vec{x}_4$ . To evaluate the influence of truss height, a parametric study was used where the height  $H$  assumed the values of  $L/10, L/15$ , and  $L/20$ .

The generic design variable  $\vec{x}_i$  represents the cross-sectional area of the truss section, for each group of bars a certain design variable was adopted:  $\vec{x}_1$  for the bottom chord,  $\vec{x}_2$  for the top chord,  $\vec{x}_3$  for the vertical bars, and  $\vec{x}_4$  for the diagonal bars.

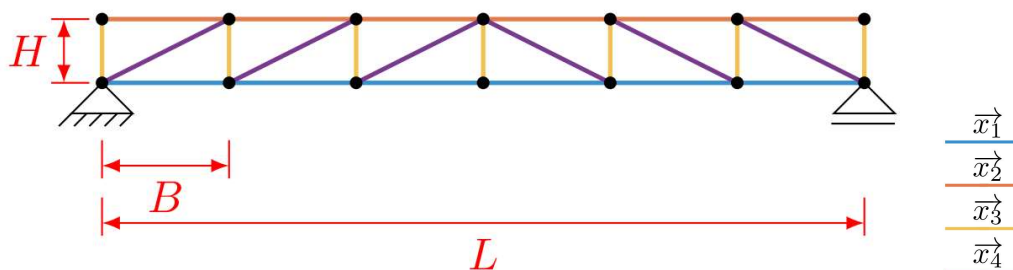


FIGURE 1. Generic representation of the nodal distance and design projects of truss.

For the application of the optimization process, wood of the dicotyledon group belonging to the resistance class C30 was considered, whose properties are depicted in standard ABNT NBR 7190 (1997). The specifications allowed for sizing are presented in TABLE 2 and the summary of the mechanical properties of the wood is presented in TABLE 3.

TABLE 2. Specifications for the woods used in the design process.

Specification	Adopted
Class	Dicotyledonae C30
Typo of wood	Sawn
Loading class	Long duration
Humidity class	I
Equilibrium humidity	12%
Wood category	1st Category

TABLE 3. Mechanical properties of calculus.

$f_{c0,d}$ (MPa)	$f_{t0,d}$ (MPa)	$E_{c0,ef}$ (MPa)
10.29	13.36	6960

### Requests and limit states

The vertical load supported by the truss included a roof load: referring to a sandwich tile (G) of  $200 \text{ N m}^{-2}$ ; own dead load was calculated for each truss variation (DL) with the service load (S) of  $250 \text{ N m}^{-2}$  and wind suction load (W) of  $800 \text{ N m}^{-2}$ .

For the verification of limit states, based on the regulatory requirements of ABNT NBR 7190 (1997), three combinations were used, two of the Ultimate Limit State (ULS): combination 1 (1.4 DL + 1.4 G + 1.4 S); combination 2 (0.9 DL + 0.9 G + 1.05 W); and one for the Serviceability Limit State (SLS): combination 3 (1.00 DL +

1.00 G + 0.3 S + 0.2 W). Later, all OF restrictions were verified with respect to such combinations.

According to the influence area, a distance of 5 m was considered between the gantries, and the distributed loads were transformed into nodes load. The Integrated Development Environment of MATLAB® software was used for structural analysis and optimization.

**Design constraints considered**

The constraints ( $g_j(\vec{x})$ ) are expressed by the eqs (10) to (14), where  $i$  is a generic bar ( $i = 1, \dots, n_{bars}$ ),  $n_{bars}$  is the number of truss bars analyzed,  $n$  is a generic node ( $n = 1, \dots, n_{nodes}$ ), and  $n_{nodes}$  is the number of nodes of the truss bars.

$$g_j(\vec{x}) = \sigma_i / \sigma_{lim} - 1 \leq 0 \tag{10}$$

$$g_j(\vec{x}) = u_n / u_{lim} - 1 \leq 0 \tag{11}$$

$$g_j(\vec{x}) = \lambda_i / \lambda_{lim} - 1 \leq 0 \tag{12}$$

$$g_j(\vec{x}) = A_{min} / A_i - 1 \leq 0 \tag{13}$$

$$g_j(\vec{x}) = b_{min} / b_i - 1 \leq 0 \tag{14}$$

Equation 10 considers the ULS checking the action of normal stresses ( $\sigma_i$ ) (traction or compression), where  $\sigma_{lim}$  is the normal stress limit.

Equation 11 is used to check the SLS, where  $u_n$  is a nodal displacement and  $u_{lim}$  is the displacement limit,

$u_{lim} = L/200$  (ABNT NBR 7190, 1997), where  $L$  is the span of the structural system.

Equation 12 represents the geometric limits of the bars based on the slenderness index ( $\lambda_i$ ), where  $\lambda_{lim}$  is the limit slenderness index, according to the standard ABNT NBR 7190 (1997), with 140 as the maximum value.

The geometric constraint resulting from the ratio between the cross-sectional area of a bar ( $A_i$ ) and the minimum area ( $A_{min}$ ) is expressed by [eq. (13)], where 50 cm<sup>2</sup> is the minimum cross-sectional area allowed (ABNT NBR 7190, 1997).

Finally, [eq. (14)] expresses the geometric constraint associating the bar thickness ( $b_i$ ) and the minimum thickness ( $b_{min}$ ), given that the standard ABNT NBR 7190 (1997) limits minimum thickness for the main parts by 5 cm.

**RESULTS AND DISCUSSION**

In this section, the results of the truss optimization process are discussed and presented in TABLE 4. These values comprise the results of thirty executions of the optimization algorithm, where  $W_{max}$  and  $W_{min}$  represent the maximum and minimum values of the penalized OF, respectively, the amplitude (A), medium ( $\mu$ ), average ( $\bar{x}$ ), standard deviation ( $\sigma$ ), and feasibility rate (TF) represents the ratio of the number of tests satisfying all constraints and the number of tests performed. To summarize the results, identification was adopted for trusses of the type x-y-L/z, where “x” is the truss typology (H for truss Howe) and “y” is the truss span in meters (6, 9, 12, and 15), and “z” for the relationship H=L/z (10, 15, and 20).

TABLE 4. Summary of the results obtained from the truss optimization process.

Truss	$W_{max}$ (kg)	$W_{min}$ (kg)	A (kg)	$\mu$ (kg)	$\bar{x}$ (kg)	$\sigma$ (kg)	TF (%)
H-6-L/10	148.9771	106.7069	42.2703	116.3885	119.0252	9.1675	100
H-6-L/15	118.7732	97.8061	20.9671	106.3101	107.3664	5.6493	100
H-6-L/20	125.1609	95.4152	29.7457	113.7032	112.5430	6.8704	100
H-9-L/10	245.1870	168.5507	76.6363	206.8425	205.9876	17.2656	100
H-9-L/15	240.8623	175.9630	64.8993	208.7818	206.8520	17.8703	100
H-9-L/20	284.3665	238.2227	46.1438	261.7093	260.3088	12.0192	100
H-12-L/10	413.3496	322.7571	90.5925	361.5206	362.0176	29.7980	100
H-12-L/15	468.9180	265.1196	203.7984	389.5996	378.2887	57.1149	100
H-12-L/20	545.2604	304.9837	240.2767	425.1910	413.7167	45.3212	100
H-15-L/10	625.4143	510.1786	115.2357	555.2714	556.3199	30.6610	100
H-15-L/15	653.5657	387.0949	266.4707	511.3104	525.7424	54.3117	100
H-15-L/20	594.3057	411.7221	182.5837	550.7577	528.0167	53.5438	100

The box plot (FIGURE 2) shows the weight change for each truss. For larger spans, the dispersion of the result increased as the increasing span also increased the loads, making the application of the optimization method more difficult.

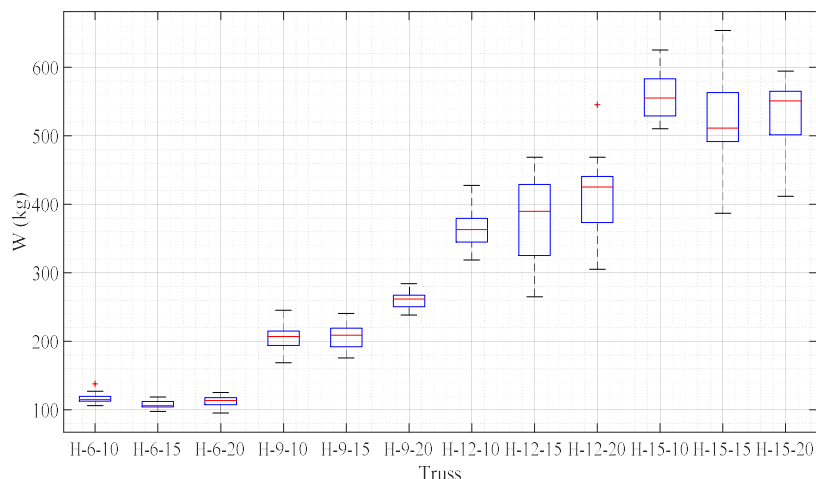


FIGURE 2. Box plot of the minimum weight (W) of the trusses.

Post the optimization process, the design variable values were obtained for each truss, with regard to the established design constraints, including the best result

with a 100% feasibility rate. For this purpose, a summary of the design variables from the truss results is presented in TABLE 5.

TABLE 5. Summarization of design variables.

Truss	Design Variables			
	$x_1$ (cm <sup>2</sup> )	$x_2$ (cm <sup>2</sup> )	$x_3$ (cm <sup>2</sup> )	$x_4$ (cm <sup>2</sup> )
H-6-L/10	57.5	57.5	57.5	56.25
H-6-L/15	57.5	57.5	57.5	57.5
H-6-L/20	56.25	56.25	75	57.5
H-9-L/10	56.25	72.45	75	56.25
H-9-L/15	100.8	93.75	62.5	100.8
H-9-L/20	112.5	112.5	78.75	75
H-12-L/10	93.75	93.75	62.5	86.25
H-12-L/15	62.5	57.5	75	112.5
H-12-L/20	87.5	80	56.25	125
H-15-L/10	125	115	62.5	115
H-15-L/15	78.75	72.45	78.75	125
H-15-L/20	187.5	75	62.5	56.25

Subsequently, the OF (W) was evaluated as a function of the span (L), for the conditions delimited in the present study (FIGURE 3).

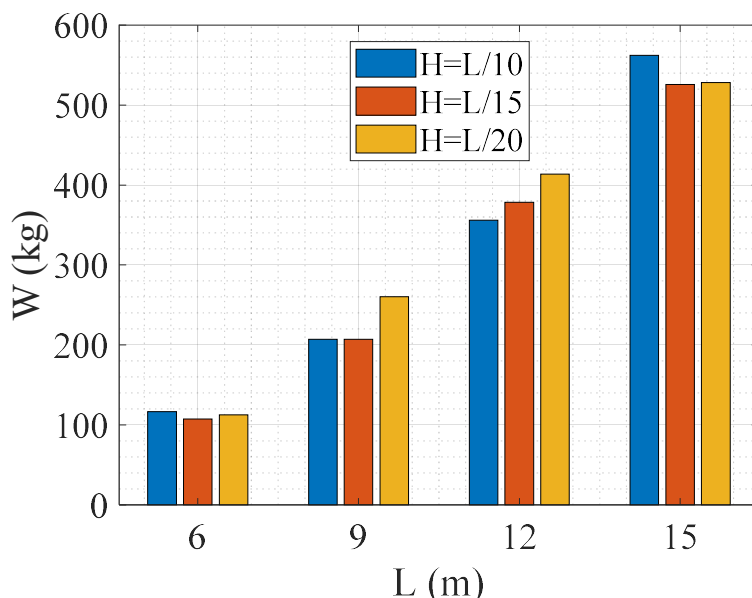


FIGURE 3. Bar plot minimum weight (W) of trusses as a function of span (L).

When assessing FIGURE 3, it was observed that the variation in the height (H) has a direct connection with the minimum weight, accentuated for trusses with spans of 9 and 12 m, implying that higher trusses were heavier with a variation of 25.84% and 16.21%, respectively. For the spans of 6 and 15 m, the change in the truss height showed lower significance in relation to the trusses with the other spans, where the truss with height L/10 resulted in heavier weights and the L/15 and L/20 returned close results

regarding to minimum value, with a variation of 8.70% and 6.95%, respectively.

Despite the difference between 6.95% and 8.70% weight variations, the height proportions resulted in structural systems satisfying the limit state equations adopted for the design problem.

Once the total weight of the trusses was evaluated, the maximum truss displacement was determined to ensure the use of the structure in service.

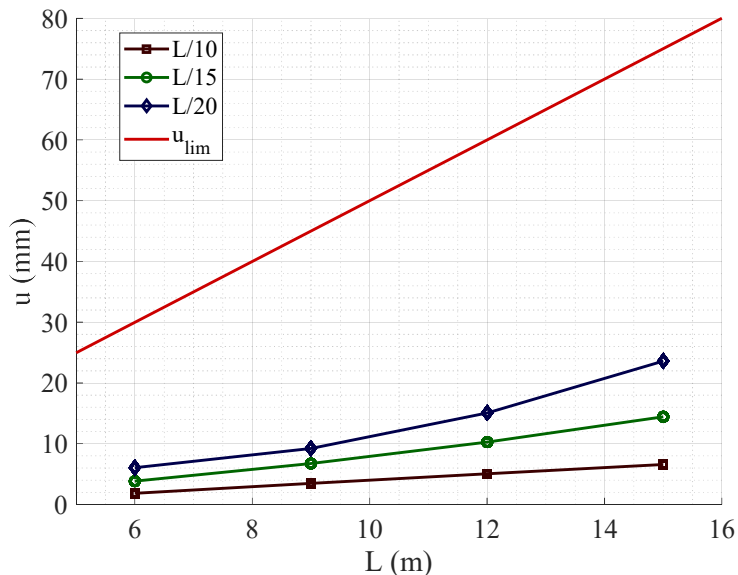


FIGURE 4. The curves maximum displacement as a function of span (L).

In relation to displacement, all trusses were within the range established by the standard ABNT NBR 7190 (1997), and according to the curve values, trusses with height L/10 showed lower displacements, with those of L/15 and L/20 demonstrated 94% and 258% higher displacements in relation to truss with height L/10, respectively.

The optimal response convergence curves among the weights of the trusses with heights L/10, L/15, and L/20 are shown in the FIGURE 5. With the increase in the span, the weight convergence occurred in numerous iterations due to increased loading causing greater complexity in the optimization process.

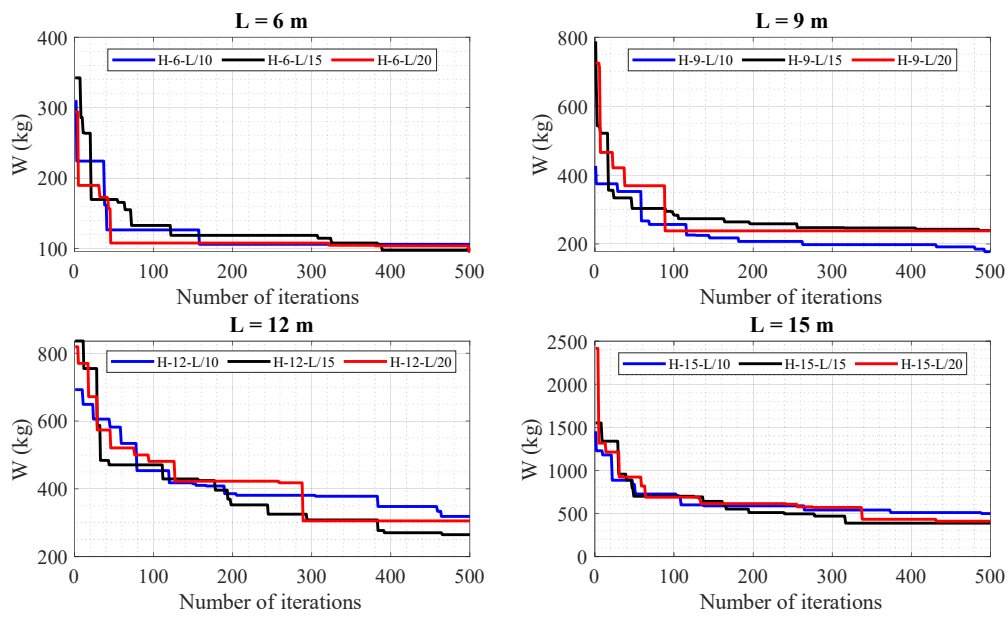


FIGURE 5. Convergence curves for minimum weight (W) of trusses.

**Evaluation of stress constraints**

To evaluate the distribution capacity of the normal truss loadings, the results of normal stress constraints were evaluated and presented in [eq. (10)] and combination 2 (ULS combination considering the wind load with variable load).

TABLE 6 demonstrates the number of samples (N), average ( $\bar{x}$ ), standard deviation ( $\sigma$ ), and confidence interval (CI) for trusses, regarding combination 1 (ULS combination considering the service load with variable load) and combination 2 (ULS combination considering the wind load with variable load).

TABLE 6. Summary of the results of normal stress constraints of trusses.

Truss	N	$\bar{x}$	$\sigma$	CI of 95%
H-6-L/10	50	- 0.7058	0.1720	(- 0.7785, - 0.6331)
H-6- L/15	50	- 0.6571	0.2135	(- 0.7372, - 0.5769)
H-6- L/20	50	- 0.6730	0.2299	(- 0.7506, - 0.5954)
H-9- L/10	50	- 0.5994	0.2165	(- 0.6721, - 0.5267)
H-9- L/15	50	- 0.6242	0.2235	(- 0.7043, - 0.5441)
H-9- L/20	50	- 0.6321	0.2395	(- 0.7097, - 0.5545)
H-12- L/10	50	- 0.5095	0.2836	(- 0.5822, - 0.4368)
H-12- L/15	50	- 0.4530	0.3457	(- 0.5331, - 0.3729)
H-12- L/20	50	- 0.5061	0.3498	(- 0.5838, - 0.4285)
H-15- L/10	50	- 0.4703	0.3389	(- 0.5430, - 0.3976)
H-15- L/15	50	- 0.4461	0.3393	(- 0.5263, - 0.3660)
H-15- L/20	50	- 0.5366	0.2778	(- 0.6142, - 0.4590)

As presented in [eq. (10)], the closer to zero the constraint result, the closer the normal stress is to the limit established by the standard. Based on the results of Table 6, the trusses of 6, 12, and 15 m span and the trusses of height L/15 demonstrated better distribution of normal stress loads, and the trusses with 9 m span those with height L/10 showed the best normal stress load distribution, using more load capacity of the structure.

**Evaluation of displacement constraints**

To evaluate the distribution capacity of the maximum displacements of the trusses, it is necessary to evaluate the results of the maximum displacement constraints, presented in [eq. (11)].

TABLE 7 shows the number of samples (N), average ( $\bar{x}$ ), standard deviation ( $\sigma$ ), and CI for the trusses for combination 3 (SLS combination).

TABLE 7. Summary results of constraints of displacement of trusses.

Truss	N	$\bar{x}$	$\sigma$	CI of 95%
H-6-L/10	14	-0.7574	0.1875	(- 0.9171, - 0.5976)
H-6-L/15	14	-0.6253	0.3075	(- 0.7951, - 0.4556)
H-6-L/20	14	-0.5568	0.3476	(- 0.7346, - 0.3789)
H-9-L/10	14	-0.6356	0.3156	(- 0.7953, - 0.4758)
H-9-L/15	14	-0.6414	0.2961	(- 0.8112, - 0.4717)
H-9-L/20	14	-0.628	0.3042	(- 0.8058, - 0.4501)
H-12-L/10	14	-0.618	0.3294	(- 0.7778, - 0.4583)
H-12-L/15	14	-0.5442	0.2973	(- 0.7139, - 0.3744)
H-12-L/20	14	-0.4946	0.3477	(- 0.6724, - 0.3167)
H-15-L/10	14	-0.6509	0.3344	(- 0.8106, - 0.4911)
H-15-L/15	14	-0.4688	0.3607	(- 0.6386, - 0.2991)
H-15-L/20	14	-0.4957	0.3248	(- 0.6736, - 0.3179)

Similar to normal stress constraints, the closer to zero the result of the constraints, the closer the maximum displacement is to the limit established by the standard. Considering the results of

TABLE 7, the trusses of 6, 9, and 12 m at trusses with height L/20 presented a better displacement distribution, and for the trusses of 15 m span the one with the best displacement distribution was the L/15.

**CONCLUSIONS**

Optimization application through the FA is helpful in effectively designing the wood structures. The height variations are directly connected to the maximum displacement. The trusses with the biggest heights result in lower maximum displacements. The maximum displacement is within the limit set by the Brazilian standard for wood design (ABNT NBR 7190, 1997).

The height proportion with a larger range could be applied in future research along with shape optimization, wherein the coordinates of the joist nodes are the problem variables. In this case, it would be possible to obtain the optimal height proportion for the specific structural model. For future studies, other optimization methods could be applied along with other typologies, shape optimization, and wood from another resistance group to obtain comprehensive results and develop optimization knowledge applied to wood structures.

**ACKNOWLEDGMENTS**

This study was financed in part by the Coordenação de Aperfeiçoamento de Pessoal de Nível Superior – Brasil (CAPES) – Finance Code 001.

**REFERENCES**

Assimi H, Jamali A, Nariman-zadeh N (2017) Sizing and topology optimization of truss structures using genetic programming . *Swarm and Evolutionary Computation* 37: 90–103. DOI: <http://dx.doi.org/10.1016/j.swevo.2017.05.009>

ABNT - Associação Brasileira de Normas Técnicas (1997) Projeto de estruturas de madeira - NBR 7190 ABNT. Brasília, ABNT.

Bianconi F, Filippucci M, Buffi A (2019) Automated design and modeling for mass-customized housing. A web-based design space catalog for timber structures . *Automation in Construction* 103: 13–25. DOI: <http://dx.doi.org/10.1016/j.autcon.2019.03.002>

Chrisp TM, Cairns J, Gulland C (2003) The development of roundwood timber pole structures for use on rural community technology projects . *Construction and Building Materials* 17(4): 269–279. DOI: [http://dx.doi.org/10.1016/S0950-0618\(02\)00114-9](http://dx.doi.org/10.1016/S0950-0618(02)00114-9)

Darwish A (2018) Bio-inspired computing: Algorithms review, deep analysis, and the scope of applications . *Future Computing and Informatics Journal* 3(2): 231–246. DOI: <http://dx.doi.org/10.1016/j.fcij.2018.06.001>

Degertekin SO, Lamberti L, Ugur IB (2018) Sizing, layout and topology design optimization of truss structures using the Jaya algorithm . *Applied Soft Computing* 70: 903–928. DOI: <http://dx.doi.org/10.1016/j.asoc.2017.10.001>

Ding S, Du W, Zhao X, Wang L, Jia W (2019) A new asynchronous reinforcement learning algorithm based on improved parallel PSO . *Applied Intelligence* 49(12): 4211–4222. DOI: <http://dx.doi.org/10.1007/s10489-019-01487-4>

Gandomi AH, Yang X-S, Alavi AH (2011) Mixed variable structural optimization using Firefly Algorithm . *Computers & Structures* 89(23): 2325–2336. DOI: <http://dx.doi.org/10.1016/j.compstruc.2011.08.002>

Hens I, Solnosky R, Brown NC (2021) Design space exploration for comparing embodied carbon in tall timber structural systems . *Energy and Buildings* 244: 110983. DOI: <http://dx.doi.org/10.1016/j.enbuild.2021.110983>

Hoang ND (2019) Image processing based automatic recognition of asphalt pavement patch using a metaheuristic optimized machine learning approach . *Advanced Engineering Informatics* 40: 110–120. DOI: <http://dx.doi.org/10.1016/j.aei.2019.04.004>

- Kazemzadeh-Parsi MJ, Daneshmand F, Ahmadfard MA, Adamowski J, Martel R (2015) Optimal groundwater remediation design of pump and treat systems via a simulation–optimization approach and firefly algorithm . *Engineering Optimization* 47(1): 1–17. DOI: <http://dx.doi.org/10.1080/0305215X.2013.858138>
- Krušínský P, Gocál J, Augustínková L, Capková E, Korenková R (2017) Proportions and static Analysis of a Historical Truss in a Rural House in Vápenná Village . *MATEC Web of Conferences* 117: 00093. DOI: <http://dx.doi.org/10.1051/mateconf/201711700093>
- Kumar D, Mishra KK (2017) Portfolio optimization using novel co-variance guided Artificial Bee Colony algorithm . *Swarm and Evolutionary Computation* 33: 119–130. DOI: <http://dx.doi.org/10.1016/j.swevo.2016.11.003>
- Kuri-Morales AF, Gutiérrez-García J (2002) Penalty function methods for constrained optimization with genetic algorithms: a statistical analysis. In: Coelho CA, Alborno A de, Sucar LE, Battistutti OC. (Ed.) *MICAI 2002: advances in artificial intelligence*. Springer, p.108–117). DOI: [http://dx.doi.org/10.1007/3-540-46016-0\\_12](http://dx.doi.org/10.1007/3-540-46016-0_12)
- Li Y, Yu Y, Zhao J (2016) Construction System Reliability Analysis Based on Improved Firefly Algorithm. *The Open Civil Engineering Journal* 10(1): 189–199. DOI: <http://dx.doi.org/10.2174/1874149501610010189>
- Li Z, Li T, Wang C, He X, Xiao Y (2019) Experimental study of an unsymmetrical prefabricated hybrid steel-bamboo roof truss. *Engineering Structures* 201: 109781. DOI: <http://dx.doi.org/10.1016/j.engstruct.2019.109781>
- Mam K, Douthe C, Le Roy R, Consigny F (2020) Shape optimization of braced frames for tall timber buildings: Influence of semi-rigid connections on design and optimization process. *Engineering Structures* 216: 110692. DOI: <http://dx.doi.org/10.1016/j.engstruct.2020.110692>
- Mayencourt P, Mueller C (2020) Hybrid analytical and computational optimization methodology for structural shaping: Material-efficient mass timber beams. *Engineering Structures* 215: 110532. DOI: <http://dx.doi.org/10.1016/j.engstruct.2020.110532>
- Nguyen HQ, Ly H-B, Tran VQ, Nguyen T-A, Le T-T, Pham BT (2020) Optimization of Artificial Intelligence System by Evolutionary Algorithm for Prediction of Axial Capacity of Rectangular Concrete Filled Steel Tubes under Compression. *Materials* 13(5): 1205. DOI: <http://dx.doi.org/10.3390/ma13051205>
- Pech S, Kandler G, Lukacevic M, Füssl J (2019) Metamodel assisted optimization of glued laminated timber beams by using metaheuristic algorithms. *Engineering Applications of Artificial Intelligence* 79: 129–141. DOI: <http://dx.doi.org/10.1016/j.engappai.2018.12.010>
- Pereira Junior WM, Borges RA, Araújo DL, Pituba JJC (2021) A proposal to use the inverse problem for determining parameters in a constitutive model for concrete. *Soft Computing* 25(13): 8797–8815. DOI: <http://dx.doi.org/10.1007/s00500-021-05745-x>
- Pereira LLM, Santos DC, Moraes MHM, Gonçalves Filho GM, Ancioto Junior EM, Pereira Junior WM, Dantas MJP (2020) Estudo de Sensibilidade do Algoritmo de Colônia de Vagalumes para um Problema de Engenharia Envolvendo Dimensionamento de Treliças . *TEMA (São Carlos)* 21(3): 583. DOI: <http://dx.doi.org/10.5540/tema.2020.021.03.583>
- Ram G, Mandal D, Kar R, Ghoshal SP (2014) Design Of Non-Uniform Circular Antenna Arrays Using Firefly Algorithm For Side Lobe Level Reduction. DOI: <http://dx.doi.org/10.5281/ZENODO.1336196>
- Rauecker JCN, Junior WMP, Pituba JJ de C, Araújo D de L (2019) Uma abordagem experimental e numérica para determinação de curvas de compressão para concreto simples e reforçados com fibras de aço . *Revista Matéria* 24(3): Article 3. Available: <https://revistas.ufjr.br/index.php/rm/article/view/29530>
- Sadjadi SJ, Ashtiani MG, Ramezani R, Makui A (2016) A firefly algorithm for solving competitive location-design problem: a case study. *Journal of Industrial Engineering International*, 12(4): 517–527. DOI: <http://dx.doi.org/10.1007/s40092-016-0160-z>
- Salehi H, Burgueño R (2018) Emerging artificial intelligence methods in structural engineering. *Engineering Structures* 171: 170–189. DOI: <http://dx.doi.org/10.1016/j.engstruct.2018.05.084>
- Schietzold FN, Graf W, Kaliske M (2021) Multi-Objective Optimization of Tree Trunk Axes in Glulam Beam Design Considering Fuzzy Probability-Based Random Fields . *ASCE-ASME Journal of Risk and Uncertainty in Engineering Systems Part B: Mechanical Engineering* 7(2): 020913. DOI: <http://dx.doi.org/10.1115/1.4050370>
- Setiadi H, Jones KO (2016) Power System Design using Firefly Algorithm for Dynamic Stability Enhancement . *Indonesian Journal of Electrical Engineering and Computer Science* 1(3): 446. DOI: <http://dx.doi.org/10.11591/ijeecs.v1.i3.pp446-455>
- Tahsildoost M, Zomorodian Z (2020) Energy, carbon, and cost analysis of rural housing retrofit in different climates . *Journal of Building Engineering* 30: 101277. DOI: <http://dx.doi.org/10.1016/j.jobbe.2020.101277>
- Talatahari S, Gandomi AH, Yun GJ (2014) Optimum design of tower structures using Firefly Algorithm . *The Structural Design of Tall and Special Buildings* 23(5): 350–361. DOI: <http://dx.doi.org/https://doi.org/10.1002/tal.1043>
- Upadhyay P, Kar R, Mandal D, Ghoshal SP (2016) A new design method based on firefly algorithm for IIR system identification problem. *Journal of King Saud University - Engineering Sciences* 28(2): 174–198. DOI: <http://dx.doi.org/10.1016/j.jksues.2014.03.001>

Villar JR, Vidal P, Fernández MS, Guaita M (2016) Genetic algorithm optimisation of heavy timber trusses with dowel joints according to Eurocode 5. *Biosystems Engineering* 144: 115–132. DOI:

<http://dx.doi.org/10.1016/j.biosystemseng.2016.02.011>

Villar-García JR, Vidal-López P, Rodríguez-Robles D, Guaita M (2019) Cost optimisation of glued laminated timber roof structures using genetic algorithms.

*Biosystems Engineering* 187: 258–277. DOI:

<http://dx.doi.org/10.1016/j.biosystemseng.2019.09.008>

Wang H, Wang W, Zhou X, Sun H, Zhao J, Yu X, Cui Z (2017) Firefly algorithm with neighborhood attraction.

*Information Sciences* 382–383, 374–387. DOI:

<http://dx.doi.org/10.1016/j.ins.2016.12.024>

Whitley D, Dominic S, Das R, Anderson CW (1994) Genetic reinforcement learning for neurocontrol problems. *Machine Learning* 13(2–3): 259–284. DOI: <http://dx.doi.org/10.1007/BF00993045>

Yang XS (2008) *Nature-inspired metaheuristic algorithms* (1<sup>o</sup>) Luniver Press.

Yeniay Ö (2005) Penalty function methods for constrained optimization with genetic algorithms. *Mathematical and Computational Applications* 10(1): 45–56. DOI:

<http://dx.doi.org/10.3390/mca10010045>

Zhang Y, Agarwal P, Bhatnagar V, Balochian S, Yan J

(2013) *Swarm intelligence and its applications*. The Scientific World Journal 1–3. DOI:

<http://dx.doi.org/10.1155/2013/528069>